EARTH'S CRYOSPHERE
SCIENTIFIC JOURNAL

Earth`s Cryosphere, 2017, vol. XXI, No. 1, pp. 23–31 **http://earthcryosphere.ru/**

CRYOGENIC PROCESSES AND FORMATIONS

DOI: 10.21782/EC2541-9994-2017-1(23-31)

SEISMOGENIC LANDSLIDE STRUCTURE AND EVOLUTION IN THE PERMAFROST AREA OF THE ALTAI MOUNTAINS (GORNY ALTAI)

M.S. Dostovalova[1], V.V. Olenchenko[2]

[1] *Joint Stock Company "Geological company "Altay-Geo",*
52, Zavodskaya str., Mayma, Altai Republic, 649100, Russia; ya.toyma@yandex.ru
[2] *Trofimuk Institute of Petroleum Geology and Geophysics, SB RAS,*
3, Koptuga ave., Novosibirsk, 630090, Russia; OlenchenkoVV@ipgg.sbras.ru

This article presents and discusses results of multiyear observations and electrical resistivity tomography studies of one of the seismogenic landslides on the territory of Gorny Altai. The study has revealed that the landsliding occurred in 2008, during the period of enhanced seismicity of the Altai-Sayan region. This is shown to be a cirque-like landslide of complicated morphology resulted from the unconsolidated deposits movement along the permafrost table. The permafrost thicknesses predicted from geophysical data vary from 22–30 m to 10 m in fault zones. During the 2008–2015 observations, the maximum displacement of the landslide scarp was 62 m, with the annual growth of its area averaging 278 m^2 (in the range from 45 to 651 m^2/year). The landslide evolution is characterized by short-term periods of activation against the backdrop of the generally declining landslide activity. These are associated with a short-term burst of seismic activity in the region when the mean summer air temperature increased by 2.1 °C versus the multiyear norm. The results of the study allow suggesting that further growth of the mean annual and summer temperatures in the Chuya seismogenic zone of Gorny Altai will lead to activation of landsliding processes.

Seismogenic landslide, mountain permafrost, electrical resistivity tomography

INTRODUCTION

Mountainous areas, typically classified as areas of high seismic activity, are known to be primary regions of earthquake-triggered landslides and their potential, which often presents a significant threat to linear structures and settlements. In the territory of Russia, landslide hazard monitoring is run by Federal Center for State Monitoring of the Subsurface Condition (SMSC Center) responsible for assessment of activity and dynamics of landslide processes at regional and local scale, and their forecasting. There are several observation sites capable to provide annual monitoring of the landslide dynamics in the Altai Mountains area. At one of these, the landslide process development have been observed since its origination until the present time. To accomplish a comprehensive study of geocryological structure of the slope affected by landsliding, the applied geophysical techniques included electrical resistivity tomography (ERT), aiming primarily to determine the following morphometric parameters of permafrost: its upper limit or depth to permafrost table; thickness; distribution pattern.

STUDY AREA

The study area is situated in Kosh-Agach district of the Altai Republic, 4.5 km southwest of the settlement of Chagan-Uzun (Fig. 1). The studies were conducted at the Chuya observation site (Landslide No. 86) located within the seismically active Chuya zone largely controlled by active deep faults of the Kurai-Sayan structural joint accompanied by feathering lower order tectonic structures [*Platonova, 2000; Rogozhin and Platonova, 2002*]. Geologically, the landslide structure of the area are confined to the fields of distribution of Neogene-Paleogene, Neogene and Quaternary deposits represented by the Karachum, Kosh-Agach, Tueryk, Beken, Kubadrin-Bashkaus Formations, Quaternary subaerial-subaquatic sediments and modern polygenetic complex.

The main horizons, most prone to deformations within both ancient and recently activated landslides are represented by Paleocene-Miocene deposits of the Kosh-Agach Formation in combination with Neogene and Quaternary deposits.

The formation is composed of gray, dark gray, greenish-gray, yellowish, brown clays, siltstone, silty

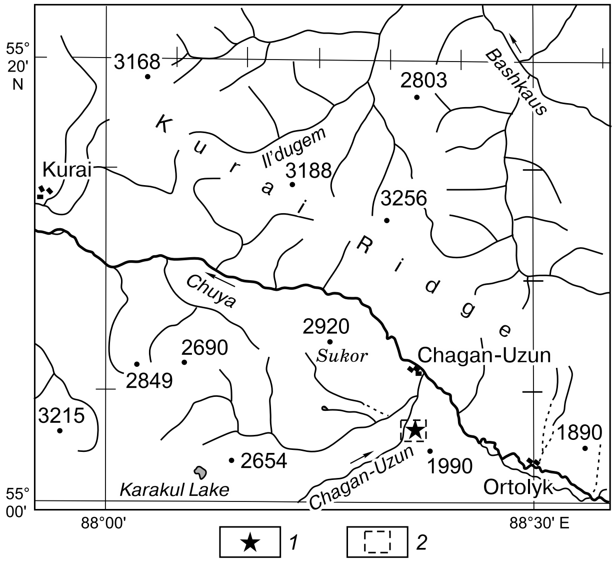

Fig. 1. Map of the area of works:

1 – study site; *2* – satellite imagery contours.

clay, sandy clays, sand, gravel and conglomerates of lacustrine, alluvial-lacustrine and lacustrine-palustrine genesis, interspersed with lenses and interlayers of brown coal and lignite; their thickness ranges from 0.05 to 9 meters. These occasionally include siderite as nodules and horizons. Given that the Kosh-Agach Fm sedimentary complex occurs generally within tectonic blocks confined to the main fault structures of the Kurai suture zone, the Kosh-Agach Fm deposits appear to be largely exposed to small amplitude seismic and neotectonic events, which is corroborated by the extensive development of tectonic breccia, travertine and greisens, as well as secondary seismic dislocations, including those formed in recent years (modern dislocations).

In terms of geocryology, the study area is classified as area of alpine (mountain) permafrost distribution with its pattern varying in line with the altitudinal zoning law, grading from the island to discontinuous and continuous type, with the increasing altitude [*Shats, 1978*]. Alpine permafrost thickness tends to grow with altitude and constitutes 25 m at 1780 m a.s.l., 65 m at 1850 m, 160 m at 1930 m and 400 m at 2920 m a.s.l. [*Shats, 1978*]. Permafrost temperature varies from – 0.2 to – 1.8 °C in the Chuya Basin [*Dostovalova, 2006*], and to – 5 °C on the northern slope exposure in the vicinity of Sukor Mt. [*Shats, 1978*]. The upper limit of permafrost occurs at a depth of 3–12 m, depending on the lithological composition of rocks and water content of the active layer (AL). Maximal AL thickness (up to 12 m) is displayed by hard rocks, while its minimum (1–4 m) is representative of coarse clastic rocks [*Piatnitskii and Pavlov, 1981*].

In the course of the monitoring research at the Chuya observation site, permafrost was often observed in the landslide scarps where frozen rocks were penetrated at a depth of 1.3–3 m from the surface. Permafrost was typically represented by clay loams and sand loams, sandy-gravel sediments with ice-rich cement and often included lenses of ice. More over, permafrost was also encountered at the bottom the transverse cracks in the landslide body, with full depth from 0.7 to 1.2–1.5 m. In this case, rocks filing the cracks had dominantly plastic and flowable consistency.

LANDSLIDE STRUCTURE AND EVOLUTION

Activation of landsliding processes reported at the Chuya observation site in summer of 2008 was evidenced by the seven newly triggered landslides within the eastern flank of the Chagan-Uzun block, a major seismogenerating structure of the 2003 Chuya earthquake. Landslide No. 86 originated on the right side of the Chagan-Uzun river (Fig. 2), to evolve into a cirquelike slump landslide of complex morphology with elements of glacier landsliding, with coverage area of 5945 m^2 (Fig. 3). Permafrost rocks up to 4.5 m thick, showing lenses of pure ice were exposed in the vertical surface of separation (Fig. 4).

The landslide inception mechanism consisted in sliding unconsolidated debris with elements of viscous wet stream flow. Estimated thickness (derived from the height of the surface of separation) of the landslide body was 4–6 m. In 2008, the area of the landslide toe was impassible due to very viscous rock-mass formed by a bulge of material. Excessive wetting of rocks at the upper limit of permafrost and at the base of the surface of separation triggered micro-events of viscous flow in the near-slope depression and landslide toe. Judging from the height of the front and side scarps, the landslide thickness ranges between 4 and 7 m in the zone of accumulation.

The surface of separation has a complex configuration consisting of several arches and scarps up to 5–6 m high, of which vertical (up to 4 m) occur in the upper part, while at the bottom part, they are covered by talus or slumping mass. The vertical part of the head scarp exposed:

– silty sands with gravel material – up to 10 % (fQ_{III}) – 1.1 m;

– layered silty sands, weakly wetted with smears of silty medium fine gravel brown soils and brownish-brown inclusions, sometimes with the presence of small shells (ka Pg_3–N_1 – Kosh-Agach Formation) – 1.2 m;

– equivalent sand loams, brownish-brown and yellow-brown, perennially frozen, hard frozen with layered cryotexture, sometimes with lenticules of pure ice (10–15 cm), gravitating toward the AL base (Kosh-Agach Formation) – 1.5 m.

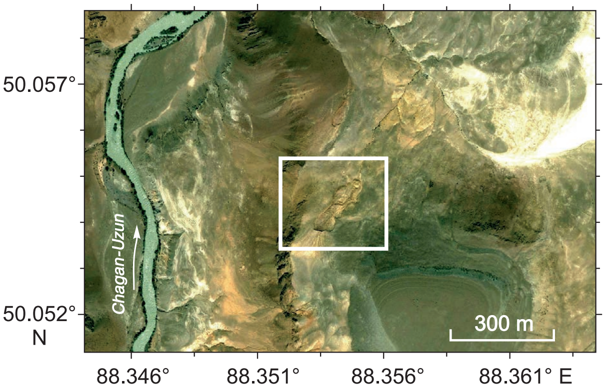

Fig. 2. Satellite image of area of landslide occurrence (http://www.bing.com/mapspreview).

Fig. 3. Landslide view in 2008 (photograph by M.S. Dostovalova).

In 2008, the permafrost table was documented in the surface of separation of the landslide at a depth of 1.5–2.3 m. Frozen deposits represent by themselves hard frozen sand loam with layered cryotexture containing ice-rich cement, with lenses of pure ice without inclusions. Thickness of the permafrost layer exposed in the main scarp ranged between 1 and 1.5 m. The scarp base and the adjacent slope depression contained viscous and fenny, soft- and high plasticity thawed soils slumping from the surface of separation and thus landsliding processes were interpreted to be thaw slumps (mud flows).

The initial stage of landsliding lies within the 1885–1930 m orographic interval, with the height difference of 45 m. The landslide formed on northern exposure of the slope with weakly pronounced debris flow scour channel; the slope angle range from 12 to 20°. The vegetation type is semidesert.

The landslide surface is for the most part structureless, flattened in the slope depression and in the viscous flow scour channel, small – blocked in the breakaway zone, while it is hollow-ridged in the landslide toe.

Water-ingress is manifested in the thawed high viscosity soils at the base of the head scarp, mud lakes in the near-slope depressions, and along the interior joint of minor scarps. Soft high-plastic soils were encountered in viscous flow scour channels. In some years of observations, the slope depressions exhibited cryogenic – pressurized low-yield sources, forming mud puddles with a diameter not greater than 0.5 m. Water head in such sources constitute first centimeters above the surface. As a rule, they experience short-term periods of activation, sometimes lasting not longer than a day. Judging by the bluish-gray or dark-gray color of clay suspensions, these sources capture subpermafrost or interpermafrost aquifers confined to clay loam and silty-sand sediments of the Paleogene-Neogene age.

Fig. 4. Exposed icy layer in the top portion of main scarp of landslide (height of the main scarp: 4–5 m). Photograph by M.S. Dostovalova, 2008.

GEOELECTRIC SECTIONS OF THE LANDSLIDE

In 2014, electrical resistivity tomography (ERT) surveys were conducted in the study area, in order to clarify its geocryological structure. Electrical tomography is an advanced modification of the vertical electrical sounding (VES) method and comprise elements of sounding and profiling [*Bobachev et al., 2006; Loke, 2009*]. The measurements were performed by the "SKALA-48" multielectrode station whose sequence of electrode combinations is equivalent to the Schlumberger and dipole-axial configurations [*Balkov et al., 2012*]. In this study, the sounding was performed to a depth of 35 m.

The data processing consisted in solving the inverse problem of resistivity sounding using Res2Dinv program in a two-dimensional model [*Loke, 2009*] and resulted in building two-dimensional sections of

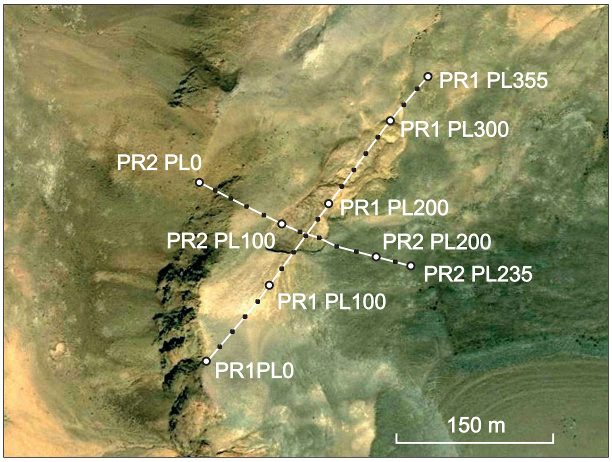

Fig. 5. ERT profiles layout (satellite imagery from http://www.bing.com/mapspreview).

electrical resistivity of rocks along the profiles (geoelectric sections) traversing the landslide structure in the longitudinal and across direction. The ERT profiles layout is shown in Fig. 5.

Figure 6 shows the profile of geoelectric section 1. The section shows the anomalously high (120–380 Ohm·m) electrical resistivity (ER) indicating a geoelectrical image of lenses of very ice-rich rocks exposed in the landslide scarp (notation *1* in Fig. 6). The lens length along the strike is about 25 m, with a thickness of about 5 m. Slumping masses (*2* to Fig. 6) are in the thawed, water-logged state in the cirque, and are characterized by low resistivity (25–45 Ohm·m). Depleted mass of the landslide toe (*3* in Fig. 6) have high resistivity (60–70 Ohm·m) compared to the water-logged rocks in the cirque indicating their lower moisture content.

The low resistivity values of thawed (10–100 Ohm·m) and frozen rocks (100–500 Ohm·m) in the upper part of the section are caused by their finely dispersed lithological composition (sand loam), while electrical properties are controlled by surface conductivity of loosely bound water films [*Frolov, 1998*]. The main slip surface (failure plane) of slumping mass sliding along the permafrost base is shown by dotted line on the section. According to the geophysical data, its occurrence depth is estimated to be 5–7 m.

The high resistivity (400–4500 Ohm·m) rocks occurring at the base of the landslide cirque (*4* in Fig. 6), much like other representative high resistivity areas tend to be tabular in shape, which may be an indication of the permafrost bedrock. The thickness of the frozen strata is found to be 20–22 m, which is consistent with the preliminary data on the geocryological structure of the area of works [*Shats, 1978*].

The frozen sediments of the unconsolidated polygenetic complex (*5* in Fig. 6) are characterized by resistivity ranging between 105 and 350 Ohm·m. Their thickness is estimated at 10 m on the geoelectric section. A decreased thickness of the high resistivity layer in the lower portion of the slope (the 250–290 m interval) interpreted to be perennially frozen (permafrost) stratum may be associated with a fault zone differentiated by lower resistivity (*6a* in Fig. 4).

A reduction in permafrost thickness in fault zones in the context of mountain permafrost was reported in earlier works [*Olenchenko et al., 2011; Severskiy et al., 2014*]. Another vertical fracture zone in the bedrock has been identified on the section within the 80–100 m interval of the profile (*6b* in Fig. 6). Thawed water-logged loose sediments in the stream channel (the 30–70 m interval in the profile) are characterized by a resistivity range from 8 to 18 Ohm·m (*7* in Fig. 6).

In the cross-section of the landslide area (Fig. 7), thawed water-logged landslide masses delineated in the landslide cirque (*1* in Fig. 7) are equated with lo-

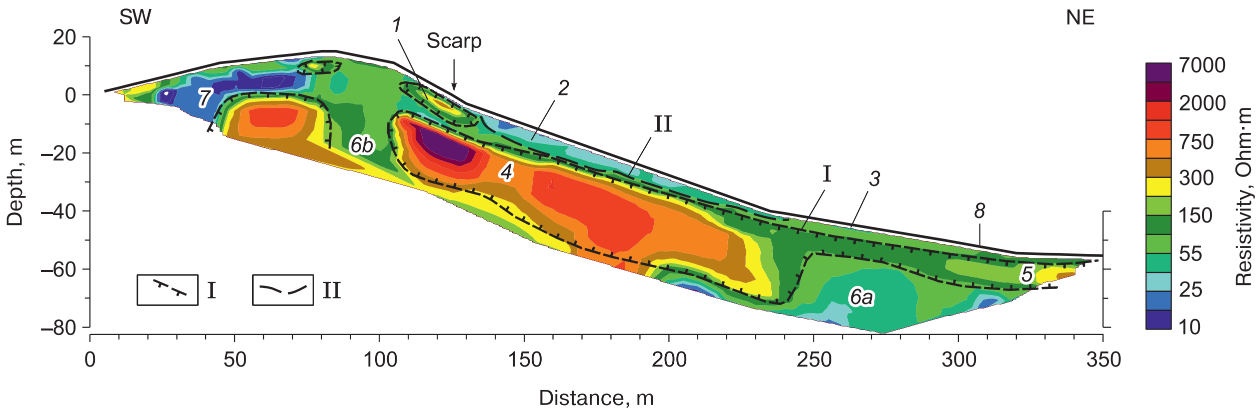

Fig. 6. Geoelectric section along profile 1:

1 – permafrost lens; *2* – water-logged slump masses; *3* – landslide toe materials; *4* – permafrost bedrock; *5* – loose permafrost deposits; *6a*, *6b* – low anomalies in resistivity within fault zones; *7* – water-logged loose deposits in debris scour channel; *8* – lower boundary of landslide. I – permafrost boundary; II – section line across main slip surface (failure plane) of landslide.

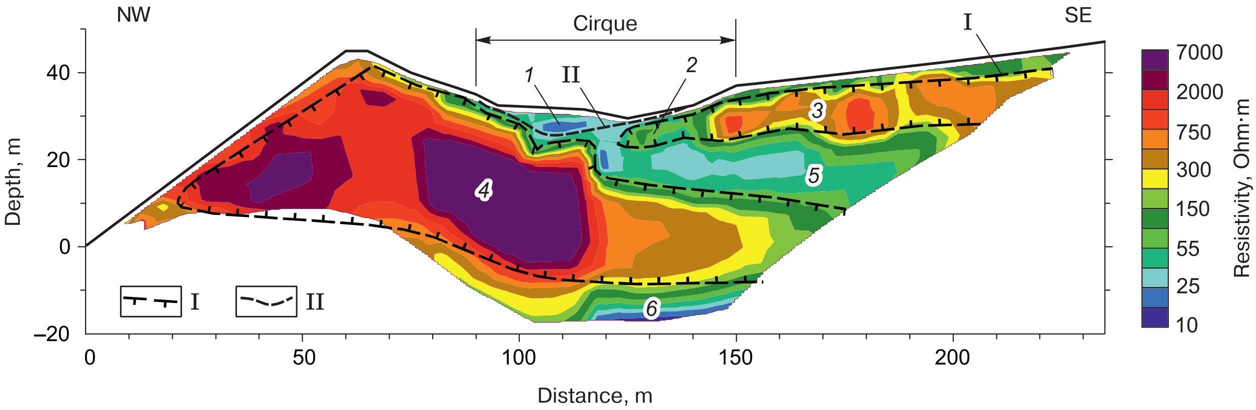

Fig. 7. Geolectric section along profile 2:

1 – water-logged slump masses; *2* – permafrost rocks at the base of landslide cirque; *3* – loose permafrost rocks of slope; *4* – bedrock permafrost; *5* – thawed loose deposits; *6* – low anomalies in resistivity within fault zone. I – permafrost boundary; II – section line across landslide failure plane.

cal low-resistivity anomaly (20–30 Ohm·m). This is where the V-shaped bottom of the cirque has south-eastern exposure, which, in combination with intensive flooding, promotes deeper thawing of the landslide cirque bottom portion. According to the geophysical data interpretation results, the thaw depth is found to be 6–8 m there. A higher resistivity (up to 100 Ohm·m) area at the base of the landslide body in the south-eastern (shady) side is interpreted as "sluggish permafrost" zone (*2* in Fig. 7). According to the geophysical data for the south-eastern slope, the thaw depth is about 2.5 meters in the cirque bed. The projected main slip surface beneath the landslide is shown by a dashed line.

The permafrost bedrock is identified as high resistivity areas (*4* in Fig. 7), which resistance varies from 300–600 to 1500–7500 Ohm·m depending on fracture intensity. Frozen loose sediments delineated in the upper part of the section (*3* in Fig. 7) show resistivity of 3000–1000 Ohm·m, and their thickness is estimated to be 18–20 m. These are underlain by thawed loose Cenozoic sediments (*5* in Fig. 7) discriminated by resistivity values between 30 and 50 Ohm·m.

The shattered rocks in the zone of the landslide occurrence are marked as a low resistivity (15–20 Ohm·m) area in the section (notation *6* in Fig. 7).

Based on the geophysical data, it has been thus established that the low resistivity slumping masses occurring atop the high resistivity interval of rocks interpreted to be permafrost. The lens of ice-rich rocks, exposed in the main scarp, has a thickness of 5 m and a length of 25 m along the strike, suggesting the landslide potential development up the slope to be 25 m. The permafrost thickness is 20 meters, whereas it is reduced to 10 m in the fault zone.

The results of sounding surveys along the transverse profile indicate that within the landslide cirque extent, the thaw depth is unevenly distributed varying from 6–8 meters on the south-eastern slope exposure to 2.5 m on the north-western exposure. The permafrost thickness is 25–30 m in the bedrock exposed in the slope, and 18–20 m within the loose deposits interval.

GEOMORPHOLOGY ANALYSIS RESULTS

The 2008 landslide schematics (Fig. 8, *A*) derived from the geomorphological survey results. The observations carried out to monitor the landslide development in the period from 2009 to 2015 included semi-instrumental measurements and GPS-mapping of the landslide limits. This resulted in building the landslide propagation schematics reflecting the process of degradation of the surface of separation and formation of a landslide thermocirque (Fig. 8, *B*). Over the 2008–2015 period the back-arc of hermocirque of Landslide No. 86 receded by 5–10 m up the slope on the eastern flank, while in the summit center its displacement constituted 18–37 m, and 50–62 m – on the western flank (Fig. 8, *B*). As such, the slope retreat was uneven, controlled by the presence of permafrost and the degree of exposure.

Maximal retreat rate is associated with the layers and lenses of permafrost exposed in the scarp on the slope of the south-western exposure. The height of minor scarps measured 5–6 m in 2008 dropped to 1–1.3 m in 2015. The previously exposed permafrost deposits have become overlain with loose material. The escarpment has been almost leveled off by the talus accumulation. Monitoring of the evolution of Landslide No. 86 showed that the activation time from its origination to dying out of the landsliding processes in the accumulation zone in the Chuya seismically active zone is spanning a period of not more than 6–10 years. Given other similar regime-forming

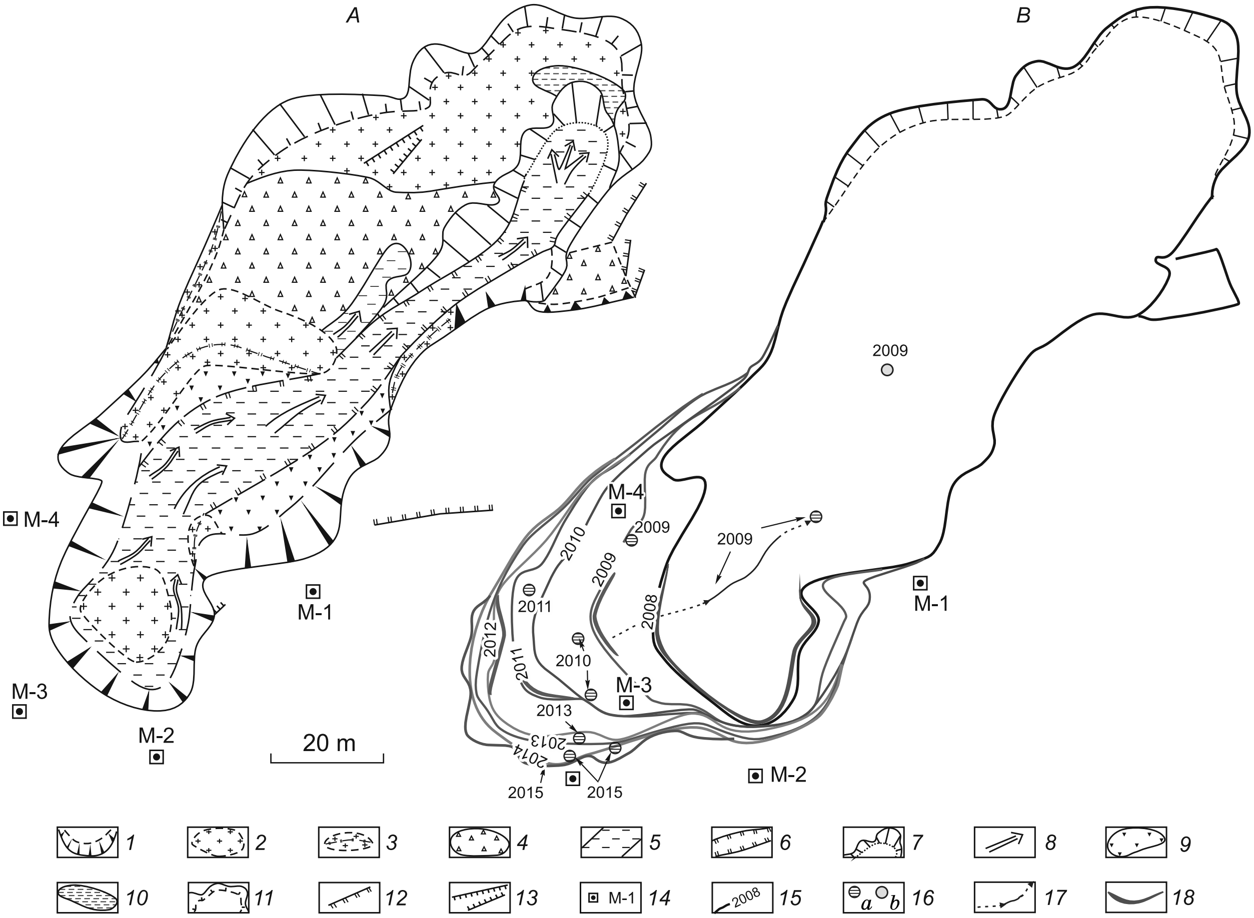

Fig. 8. Landslide (*A*) geomorphology schematics and main scarp degradation in the period of 2008–2015 (*B*).

1 – main scarp; *2* – structureless translational slide blocks; *3* – structureless translational slide ridges and swells; *4* – structural landslide blocks; *5* – mud flows (slumping mass flow); *6* – slumping mass channel with side crests; *7* – escarpment face of the thaw slump toe; *8* – direction of slumping mass flow; *9* – structureless translational slide blocks (dry gliding of landslide masses); *10* – blocked depression with mud cracks (desiccated lakelet); *11* – front face of landslide toe; *12* – tensile crack feathering landslide; *13* – trench; *14* – observational marks; *15* – main scarp contours and year of mapping; *16* – wetted soils (*a*), water ingress localions (*b*); *17* – stream flowing along the toe, mapped in 2009; *18* – permafrost lenses mapped in 2008, 2009, 2011, 2012.

factors (slope morphology, lithological composition of rocks, cryological properties of permafrost), the lower depth of landslide deposits capture is responsible for quicker extinction rates of landslide processes.

Initiated in 2008, Landslide No. 86 acquired features of low activity (suspended to dormant) landslide structure over the period of 7 years. Most evidences of a drastic decline in its activity observed during the 2014–2015 biennium have the following visual attributes of landslide mitigation: flattening of scarps and their healing with loose debris; scars in the relief of the landslide become colonized by vegetation; flattened forms of the landslide elements; washed out cracks.

Analysis of observations has shown (Table 1) that the landslide evolution can be divided into the following periods of activity: 2008 – a year of landslide inception (triggerring); 2009 – a year of active retreat of the back-arc of the landslide scarp and development of thermocirques at maximal retreat rates; 2012 – the year of ultimate activation of landslide processes against the backdrop of the progressively declining activity of the landslide; 2015 – a year of minor activation of landslide processes against a steady decline of landsliding processes. Notably, according to the Altai-Sayan Branch of Geophysical Survey SB RAS data, in those same years seismic processes intensified in the Altai-Sayan region and, specifically, in the territory of the Altay Republic, which was evidenced by the increasing number of appreciable seismic events (of magnitude (M) 3 and above) including M = 5 and above earthquakes.

A series of moderate to strong events (M > 5.0) took place in the Altai-Sayan region (ASR): in the Republic of Tyva (M = 5.2) and in Irkutsk region

Table 1. **Results of observations on Landslide No. 86**

No.	Activation indicator	2009	2010	2011	2012	2013	2014	2015	2008–2015*
1	Height of vertical scarp (in 2008: 4.5 m)	3.8	2.7	2.7	2.8	2.1	1.2	1.35	–
	Maximum displacement of the main scarp, m:								
2	on western flank	11.2	8.5	4.7	6.5	2.65	1.44	4.0	62.0
3	on eastern flank	5.3	1.2	1.5	1.8	0.5	0.6	0.6	10.0
4	at the top (summit)	7.9	8.2	5.3	6.2	2.1	3.2	2.35	37.0
5	Incremented in the landslide scarp area, m^2	651	476	127	430	117	100	45	1946
6	Trends in landsliding processes evolution	Max.	Decline		Growth	Decline		Growth	–
7	Activation degree	High	High	High	High	Moderate	Moderate	Moderate	–
8	Activation relative to average multiyear	Higher	Higher	Higher	Higher	The same level	The same level	A little higher	–
9	Activation relative to preceding year	Lower	Lower	Lower	Higher	Lower	The same level	Higher	–
10	Stage of propagation	Moving slump					Suspended process		–

* Distances and areas were derived from the medium accuracy GPS-mapping data. In the resulting column (2008–2015) indicators show maxima for all of the lines.

(M = 6.7) in 2008; the 2011–2012 earthquake (M = 6.5–6.7) in the Republic of Tyva. In the ASR area, altogether 15 seismic events with a magnitude of more than 5 were documented in 2012 alone (versus not more than 1 to 7 events, in other years). In the Altai Republic, M > 5 earthquakes occurred in 2012 (2 events) 2013 (1), 2014 (2), and in 2015 (1).

The air and permafrost temperature regimes constitute a critical factor in the activation of landslide processes. According to the Kosh-Agach weather station located 23 km from the research area, in 2008, during the formation of the landslide, the mean summer air temperature grew up to +14.7 °C versus its climate norm of +13.1 °C (Fig. 9). In 2012 and 2015, the average temperature during the summer period (+15.2 °C and + 15.1 °C, respectively) was also higher than normal.

In other years, the average summer temperature ranged between 12.7 and 14.5 °C. The active layer thawed to the full in 2008, in the first decade of July, in 2012 – in the second decade of July, and in other years the AL thawing was completed in late July – early August. Thawing rate can be estimated by the thaw state of soil as of April, 30. On that day, maximum thawing was observed in 2012 (79 cm), 2014 (83 cm), 2015 (98 cm), while the minimum thaw was reported for 2009 (14 cm).

The present analysis allows to identify a set of factors contributing to triggering landslide processes and forcings that govern the subsequent retreat of the surface of separation and the formation of thermocirque. The factors controlling the landslide occurrence are represented on the one hand by favorable geological and geomorphological characteristics of the area (tectonic, geomorphological, lithological and permafrost features), and on the other hand by fast-acting drivers (meteorological and seismic factors).

It should be noted that temperature regime of the area during the summer season and enhanced seismicity in the south-eastern part of the Altay Republic and its adjacent areas play a major role in triggering the landsliding processes. They also determine the stress state of the subsurface, and, in particular, that of the rocks in the aeration zone.

The triggers of the thermocirques growth are represented primarily by the summer temperature and hydrothermal regime of the active layer and permafrost rocks. Given temperature rises during the summer months, the back-arc of thermocirque advances more actively than at lower summer temperatures (Fig. 10).

The results of field observations have thus revealed that the landslide evolution runs parallel with a progressive decrease in its activity intermittent

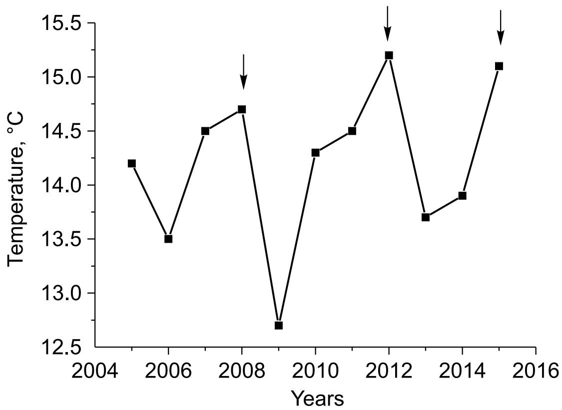

Fig. 9. Mean summer air temperatures obtained at the Kosh-Agach weather station (23 km from the object of study).

Arrows show periods of the landslide activation.

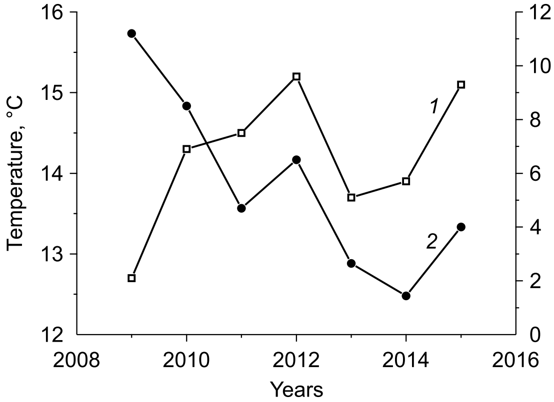

Fig. 10. Variations in mean summer air temperatures (*1*) and retreat of the back-arc of thermocirque (*2*) in westward direction over the 2009–2015 observational period.

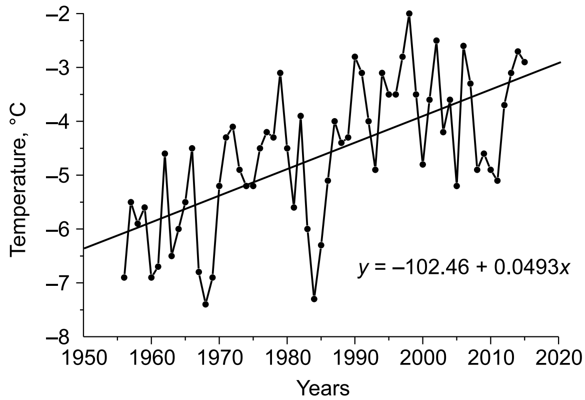

Fig. 11. Mean air temperatures in the last 60 years and approximation by linearization of their function.

with short periods of activation and is asociated, on the one hand, with an increase in seismic activity in the region and stressed state of the subsurface, and, on the other hand, with positive anomalies in the mean summer temperature.

The findings from the previous research [*Shitov and Dostovalova, 2013*] showed that that a high correlation is observed between the temperature conditions, seismic activity in the Republic of Altai and landsliding activity in the Chuiya seismically active zone, with seismic events acting as a triggering factor in the landsliding activation. The maximum correlation coefficients range between 0.43 and 0.78.

The correlation analysis also showed that the role of temperature regime tends to increase with the growing number of active (moving) and suspended landslides. This is due to the fact that most of the newly formed and moving landslides are thaw-slump type whose failure plane often coincides with the upper limit of the permafrost, or AL lower limit (alternatively, freeze/thaw boundary). In other words, hydrothermal regime of rocks in the aeration zone at the interface between active layer and permafrost plays an important role in the activation of landsliding processes.

According to the Kosh-Agach (Chuya basin) weather station data over the past 60 years, the average annual temperature has increased (warmed) with linear approximation from –6.1 to –3.2 °C (Fig. 11). It stands to reason that there is a positive correlation between the hydrothermal regime of rocks at the seasonal freeze/thaw boundary and the temperature regime of the area. In particular, both the depth of freezing of soils and their thawing rate in spring and summer season have direct relationship with positive anomalies of the air temperature. No doubt, this should involve the activation of landsliding processes in the region.

CONCLUSIONS

The field studies in combination with the geophysical investigations allowed the following inferences:

Landslide No. 86 formed during the 2008 seismic activation in the Altai-Sayany region. It represents by itself a cirquelike landslide of thaw slump type whose complex morphology includes elements of glacier landslide. The mechanism of formation of the landslide featured sliding of loose rocks with elements of the viscous wet flow along the permafrost table. Thickness of the main body of the landslide in the surface of separation is 5–6 m. The landslide formation was largely controlled by tectonic structures. The main scarp of the landslide (surface of separation) is confined to a tectonic fault detected by electrical resistivity tomography. Seismic events acted as triggering mechanism for propagation of landslides whose occurrence is localized near active tectonic faults.

Hard frozen sand loams (thickness: up to 1.5 m) with lenses of ice were exposed in the lower portion of the surface of separation. According to geophysical data, the layer of frozen ice-rich rocks has thickness of 5 m and length of 25 m along strike, which constitutes a potential for the landslide propagation up the slope.

Permafrost table exposed in the wall of separation was observed in 2008–2009 at a depth of 1.5–3.0 m above the ground surface, whereas in the subsequent years of observations its occurrence depth was established at 1.35–2.0 m. According to the ERT data, permafrost table occurs within the contours of the landslide cirque at a depth of 2.5 m on the slope of the north-western exposure to 6–8 m on the slopes of the south-eastern exposure.

The thickness of permafrost strata estimated by geophysical methods varies from 22–30 m in undisturbed bedrocks to 10 m in fault zones.

The landslide evolution pattern shows periods of short-term activation against the background of its generally declining activity. These are associated with the periods of intensification of seismic activity in parallel with positive temperature anomalies in the region.

The results and findings of this research enable to make preliminary forecast of landslide occurrence. Given the current climate warming trends and judging from the permafrost lens parameters in the main scarp, the evolution of the investigated landslide structure until the landsliding processes die out, with the retreat rate taken into account, will proceed during 5–10 years.

A comprehensive geological and geophysical study of landsliding processes and regime-forming factors by the example of one landslide allows to make short-term forecasts for further landsliding processes and to assess the risk of their hazard for engineering facilities.

References

Balkov, Y.V., Panin, G.L., Manstein, Yu.A., Nanstein, A.K., Beloborodov, V.A., 2012. Electrical resistivity tomography: tools, methodology, applications. Geofizika, No. 6, 54–63.

Bobachev, A.A., Gorbunov, A.A., Modin, I.N., Shevnin, V.A., 2006. Electrical resistivity tomography survey by resistivity and induced polarization methods. Pribory i sistemy razvedochnoi geofiziki, No. 2, 14–17.

Dostovalova, M.S., 2006. Regime-forming factors in cryogenic head flow of the Kosh-Agach settlement area flooding. Prirodnye resursy Gornogo Altaya, No. 1, 85–89.

Frolov, A.D., 1998. Electrical and elastic properties of permafrost and ice. ONTI PNTs RAN, Pushchino, 515 pp. (in Russian)

Loke, M.H., 2009. Electrical imaging surveys for environmental and engineering studies. A practical guide to 2D and 3D surveys, RES2DINV Manual [Electronic source]. – URL: http://www.abem.se/files/res/2dnotes.pdf (submittal data: 22.12.2015).

Olenchenko, V.V., Kozhevnikov, N.O., Antonov, E.Y., Pospeeva, E.V., Shein, A.N., Stefanenko, S.M., 2011. Distribution of permafrost strata in the Chuya depression (the Altai Mountains) from electromagnetic sounding data. Kriosfera Zemli XV (1), 15–22.

Platonova, S.G., 2000. Modern tectonic activity from releveling data, in: 300 years of mining-and-geological service in Russia: History of mining, geological structure and minerals of Altai: Proceedings of scientific conference (Barnaul, 14–15 Apr., 2000). Izd-vo Alt. un-ta, Barnaul, pp. 161–165. (in Russian)

Piatnitskii, V.V., Pavlov, V.V., 1981. A geotechnical and hydrogeological survey (1:50 000) report for land reclamation applications in the Chuya basin area. ZSGU, Novokuznetsk, Vol. 1, 137 pp.; Vol. 3, 121 pp. (in Russian)

Severskiy, E.V., Olenchenko, V.V., Gorbunov, A.P., 2014. The influence of local factors on the structure of permafrost Zhosalykezen Pass (Northern Tien-Shan). Earth's Cryosphere (Kriosfera Zemli) XVIII (4), 11–19.

Rogozhin, E.A., Platonova, S.G., 2002. Source zones of large earthquakes in the Altai Mountains in the Holocene. OIFZ RAN, 130 pp. (in Russian)

Shats, M.M., 1978. Geocryological conditions of the Altai-Sayany mountainous area. Nauka, Novosibirsk, 103 pp. (in Russian)

Shitov, A.V., Dostovalova, M.S., 2013. Analysis of impacts on some exogenous geological processes in the Altai Mountains. Prirodnye resursy Gornogo Altaya, No. 17, 55–66.

Received January 25, 2016